Helmholtz solitons: Maxwell's equations, interfaces, bistability & counterpropagation

P. Chamorro-Posada, J. Sánchez-Curto

Departamento de Teoría de la Señal y Comunicaciones e Ingeniería Telemática, Universidad de Valladolid, ETSI Telecomunicación, Campus Miguel Delibes s/n, Valladolid 47011, Spain;
e-mail: pedcha@tel.uva.es julsan@tel.uva.es

V. E. Grikurov

Department of Mathematical Physics, Institute of Physics, St. Petersburg University, St. Petersburg-Petrodvoretz 198504, Russia

G. S. McDonald and J. M. Christian

Joule Physics Laboratory, School of Computing, Science and Engineering, Institute for Materials Research, University of Salford, Salford M5 4WT, United Kingdom
e-mail:g.s.mcdonald@salford.ac.uk j.christian@salford.ac.uk

We give a brief overview of some new results in Helmholtz soliton theory. Firstly, fundamental considerations are made in terms of new contexts for Helmholtz solitons that arise directly from Maxwell's equations. We then detail applications of Helmholtz solitons in material interface geometries: generalising Snell's law to nonlinear beams and reporting new qualitative phenomena. Novel families of bistable soliton solutions to a cubic-quintic Helmholtz equation are also presented. Finally, an analysis of counterpropagating beams that includes new bidirectional solitons is summarized. This paper is dedicated to the late Dr. Valery E. Grikurov.

1 Introduction

Helmholtz equations provide an analytical platform for understanding oblique (off-axis) and longitudinal grating aspects of optical beam propagation. They play a key role in modelling many photonics applications since even the simplest geometries - for example, multiplexing [1] and interface configurations [2] - have intrinsically angular characters that are inaccessible from conventional (paraxial) theory.

It is now well known that, by retaining the full generality of a governing nonlinear Helmholtz (NLH) equation, one can capture scalar beam evolution at *any* angle with respect to the reference axis [3, 4]. In contrast, paraxial theory is restricted to modelling beams that each travel along, or very-nearly along, this axis. The validity of the Helmholtz approach requires $\lambda/w_0 \equiv \epsilon \ll O(1)$, where λ is the free-space carrier wavelength and w_0 is the beam waist. Since $\epsilon \ll O(1)$ must always be satisfied, one may ignore vector corrections to the governing equation that are necessary in narrow-beam regimes, i.e., where $\epsilon \sim O(1)$ [5, 6].

In this paper, we compare the predictions of Helmholtz modelling to those of Maxwell's equations. A description of soliton beams incident on material interfaces is then presented, including the report of a modified Snell's law. Next, we outline some key properties of bistable Helmholtz solitons. Finally, an asymptotic analysis of counterpropagating Helmholtz soliton beams is detailed.

2 Maxwell's Equations

A TE-polarized electric field $\mathbf{E}(x,z,t) = \widehat{\mathbf{y}}E_y(x,z,t)$ confined to a two-dimensional planar waveguide is governed by the Maxwell equations [7]

$$\frac{\partial E_y}{\partial x} = -\mu_0 \frac{\partial H_z}{\partial t} \tag{1}$$

$$\frac{\partial E_y}{\partial z} = \mu_0 \frac{\partial H_x}{\partial t} \tag{2}$$

$$\frac{\partial H_x}{\partial z} - \frac{\partial H_z}{\partial x} = \epsilon_0 \epsilon_r \frac{\partial E_y}{\partial t}. \tag{3}$$

Here, propagation takes place in the (x,z) plane. In a Kerr medium, the relative dielectric permittivity is well described by $\epsilon_r \equiv n^2 = n_0^2 + \delta_{NL}(E_y)$, where n_0 is the linear contribution to the total refractive index n. In sufficiently slow media, where the characteristic response time of the nonlinearity is much greater than the temporal period of the field oscillations, one has $\delta_{NL} \approx 2n_0^2 n_2 \langle E_y^2 \rangle$, where n_2 is the Kerr coefficient and $\langle\rangle$ denotes the time-average over many optical cycles. Such dynamics

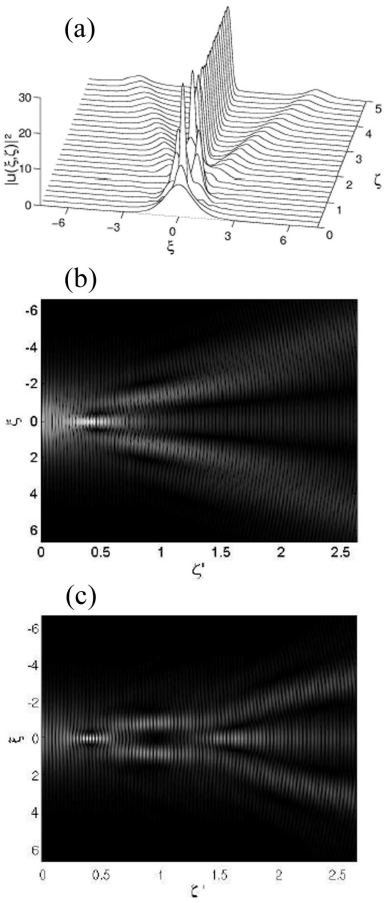

Figure 1: (a) Splitting of an $N = 3$ soliton in the NLH model. (b) The splitting phenomenon uncovered in Maxwell's equations, for an instantaneous medium nonlinearity, is accompanied by 3rd harmonic generation. (c) In a slow medium, harmonic generation is suppressed.

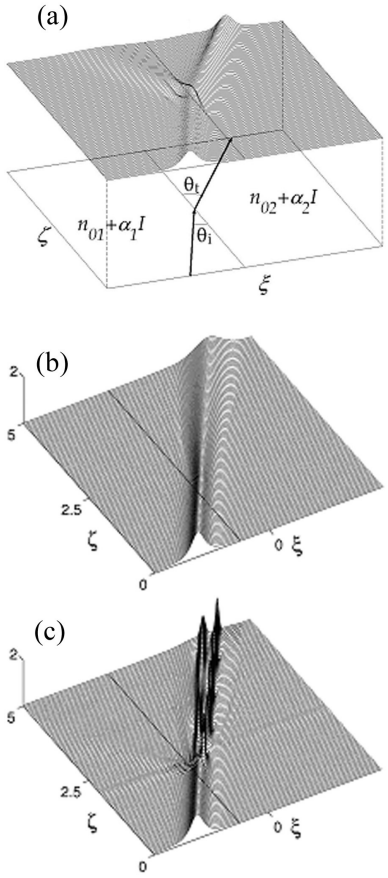

Figure 2: (a) Stable soliton refraction in a typical geometry for the material interface problem. Complex soliton evolution at the interface between two media that have the same linear refractive index, but different Kerr coefficients: (b) $\alpha_2 < \alpha_1$, and the beam undergoes diffractive broadening; (c) $\alpha_2 > \alpha_1$, and the soliton splits into several narrower solitons.

are typically modelled by a Debye relaxation equation [8].

For a continuous-wave beam $E_y(x,z,t) = \Re\{E_0 u(x,z)\exp[i(kz-\omega_0 t)]\}$, one can derive a scalar NLH equation for the (dimensionless) complex envelope u [3]:

$$\kappa\frac{\partial^2 u}{\partial\zeta^2} + i\frac{\partial u}{\partial\zeta} + \frac{1}{2}\frac{\partial^2 u}{\partial\xi^2} \pm |u|^2 u = 0. \qquad (4)$$

The normalization is $\zeta = z/L_D$ and $\xi = \sqrt{2}x/w_0$, where $L_D = kw_0^2/2$. The (inverse) beam width is quantified by $\kappa = 1/(kw_0)^2 = \epsilon^2/4\pi^2 n_0^2 \ll O(1)$, where $k = n_0 k_0$ and $k_0 = \omega_0/c = 2\pi/\lambda$. Finally, $E_0 = (n_0/|n_2|kL_D)^{1/2}$ and the $\pm$ sign flags a focusing/defocusing nonlinearity.

Helmholtz nonparaxiality acts as a perturbation that can modify the propagation properties of multi-soliton solutions of the nonlinear Schrodinger equation. For instance, during the initial focusing stages of periodic evolution, the Helmholtz operator $\kappa\partial_{\zeta\zeta}$ in Eq. (4) increases the period of a two-soliton bound state [9]. A similar effect has been confirmed by numerical solution of the full Maxwell equations [7].

When even stronger nonparaxiality is present, a launched high-order soliton can become susceptible to a fission instability, whereby the bound state breaks up into its constituents [9]. Figure 1(a) illustrates the splitting of a 3rd-order beam into three fundamental Helmholtz solitons. Figure

1(b) displays the electric field amplitude at a given instant, obtained by solving Maxwell's equations (1)-(3) and assuming an instantaneous nonlinearity. The two simulations are in good qualitative agreement, but there are noticeable differences in the detailed evolution for the two cases. These differences have been found to have their origin in the presence of parametric conversion to the third harmonic $3\omega_0$ in the strong focusing stages of the Maxwell representation. This effect provides a loss mechanism for the fundamental frequency component, thereby introducing an additional perturbation that modifies the propagation properties of the beam. Harmonic generation is omitted in Eq. (4), where only a single spectral component ω_0 is considered.

We find that third harmonic generation, and higher-order wave-mixing processes, are suppressed by a relatively slow nonlinear response. This is illustrated well in Fig. 1(c), which shows the calculated electric field amplitude at a specific time. The description of the fission process, in the region of space shown in Fig. 1(c), is in excellent agreement wih the results obtained using scalar model (4). Nevertheless, the detailed temporal evolution exhibits rich dynamics that are determined by the choice of medium response time. This scenario contrasts strongly with evolution in an instantaneous medium.

3 Solitons at Interfaces

The oblique incidence of solitons at the boundary separating two Kerr-type dielectrics [see Fig. 2(a)] can be well-described by a Helmholtz model [2]. The interface is characterized by the parameters (n_{01}, α_1) and (n_{02}, α_2), where n_{0i} and α_i $(i = 1, 2)$ are the linear refractive indices and Kerr coefficients, respectively, so that u is governed by

$$\kappa\frac{\partial^2 u}{\partial\zeta^2} + i\frac{\partial u}{\partial\zeta} + \frac{1}{2}\frac{\partial^2 u}{\partial\xi^2} + |u|^2 u = \left[\frac{\Delta}{4\kappa} + (1-\alpha)|u|^2\right] H(\xi)u, \quad (5)$$

where H is a Heaviside function, $\Delta \equiv 1-(n_{02}/n_{01})^2$ and $\alpha \equiv \alpha_2/\alpha_1$.

Simulations show that, when there is a mismatch in only the linear part of the refractive index, the incident solitons are governed by Snell's law. In general, soliton beam reflection and refraction characteristics possess key features that cannot be adequately described by paraxial theory. We have found that the classic Snell's law (for linear plane waves) also applies to such nonlinear beams when it is supplemented by a parameter γ, so that

$$\gamma n_{01}\cos\theta_i = n_{02}\cos\theta_t, \quad (6)$$

where θ_i and θ_t are the angles of incidence and refraction, respectively, measured with respect to the interface, and

$$\gamma = \left[\frac{1+2\kappa\eta_0^2}{1+2\kappa\eta_0^2\alpha(1-\Delta)^{-1}}\right]^{1/2}. \quad (7)$$

Here, we also report new behaviour when the linear refractive index is continuous across the interface. When a soliton enters a medium with a weaker nonlinearity ($\alpha_2 < \alpha_1$), the outgoing beam may suffer diffractive spreading without limit - unless the input power exceeds some critical value [see Fig. 2(b)]. However, when the second medium is characterized by a stronger nonlinearity ($\alpha_2 > \alpha_1$), excess power associated with the incident soliton can cause the beam to break up into a distribution of narrower solitons [see Fig. 2(c)].

The Helmholtz model of interface geometries (5) yields important quantitative corrections to paraxial predictions [10, 11] that can exceed 100% [2]. Moreover, significant qualitative differences between the two descriptions appear when $\alpha_2 > \alpha_1$. In the paraxial regime, the number of secondary solitons increases depending on γ. Helmholtz modelling shows that a more restrictive number of solitons is actually created. We also find that the multi-soliton structure that develops depends not only on the aforementioned index relationship, but also on θ_i.

4 Bistable Solitons

A more general class of dielectric media is described by $\delta_{NL}(E_y) \approx 2n_0^2\left(n_2E_y^2 + n_4E_y^4\right)$. For this model, the governing NLH equation is [12]

$$\kappa\frac{\partial^2 u}{\partial\zeta^2} + i\frac{\partial u}{\partial\zeta} + \frac{1}{2}\frac{\partial^2 u}{\partial\xi^2} + |u|^2u + \alpha|u|^4u = 0, \quad (8)$$

where $\alpha \equiv n_4|E_0|^2/n_2$. We have derived exact analytical solitons to Eq. (8) that capture the generic features expected for Helmholtz solutions [i.e., features of κ-type, $\kappa \times$ *intensity*-type, and $\kappa \times (velocity)^2$-type]. The known paraxial solutions [13, 14] can be recovered by enforcing a simultaneous algebraic multiple limit. This limit corresponds

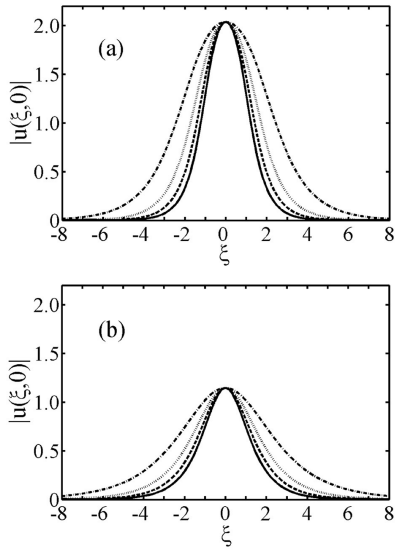

Figure 3: Angular beam broadening for (a) upper- and (b) lower-branch Helmholtz solitons. Solid: $\theta = 0°$ (paraxial), dashed: $|\theta| = 30°$, dotted: $|\theta| = 45°$, dot-dashed: $\theta = 60°$. The paraxial profile is insensitive to $|\theta|$.

to the slowly-varying envelope approximation, and it is thus formally equivalent to $\kappa\partial_{\zeta\zeta} \to 0$.

A key quantity is the product $2\kappa V^2 = \tan^2\theta$, where V is the conventional transverse velocity parameter and θ is the propagation angle of the beam relative to the z direction [3]. As $|\theta|$ increases, the projected beamwidth measured in the (x, z) frame also increases, irrespective of both κ and the system nonlinearity (see Fig. 3). In paraxial modelling, one must always respect $2\kappa V^2 \ll O(1)$. For moderate and large angles, where $2\kappa V^2$ is no longer negligibly small, we have uncovered corrections to paraxial theory that can exceed 100%. Thus, off-axis propagation alone can define a type of angular nonparaxiality, where $0 < 2\kappa V^2 \leq \infty$ (equivalent to $0 < |\theta| \leq 90°$) in such a way that the narrow-beam inequality $\kappa \ll O(1)$ is always preserved.

When $\alpha < 0$, one can identifiy pairs of solutions that possess the same (intensity) half-width-at-half-maximum but have different peak intensities (see Fig. 4). Such solutions appear to be the first reported bistable Helmholtz solitons [12]. Extensive numerical simulations have shown that soliton states lying on both solution branches are robust against perturbations.

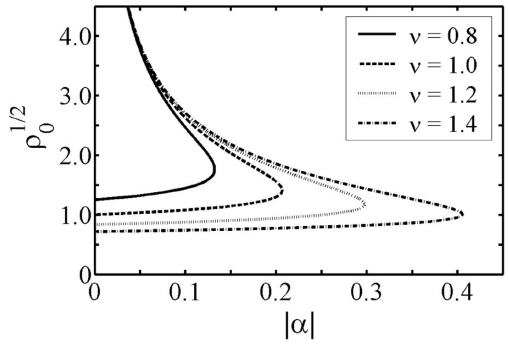

Figure 4: Bistable solution families relating the beam peak amplitude $\rho_0^{1/2}$ to the material parameter $\alpha < 0$. The parameter ν determines the half-width of the normalized intensity distribution in units of $\Delta \approx 0.77$.

5 Counterpropagation Solitons

Counterpropagating beams have been routinely described within the framework of paraxial theory [15, 16]. A Helmholtz treatment can be more appropriate either because of inherent angular geometry [1] or to account for longitudinal grating effects. The new asymptotic analysis here uncovers novel counterpropagating solitons of NLH equations.

By substituting $u(\xi, \zeta) = \psi(\xi, \zeta)\exp(-i\zeta/2\kappa)$ into Eq. (4), one transforms from a forward reference frame to one that is essentially stationary. One finds

$$\kappa\frac{\partial^2\psi}{\partial\zeta^2} + \frac{1}{4\kappa}\psi + \frac{\partial^2\psi}{\partial\xi^2} + F\left(|\psi|^2\right)\psi = 0, \quad (9)$$

where $F(|\psi|^2)$ is any smooth nonlinearity function for which $F(0) = 0$. For simplicity, a re-scaling of $\sqrt{2}\xi \to \xi$ has been implemented in Eq. (9). Since $\kappa \ll O(1)$, a perturbative analysis is performed using κ as an expansion parameter. We investigate asymptotic solutions to Eq. (9) of the form:

$$\psi(\xi, \zeta) = \psi_0(X, \zeta)\cos\Theta + \sum_{j=1}^{\infty}\kappa^j\psi_j(\xi, \zeta; Z), \quad (10)$$

where $\Theta \equiv Z + \phi(\xi, \zeta)$, $X = \xi - v\zeta$, v is a transverse speed, and $Z = \zeta/2\kappa$. Here, ψ_0 and $\{\psi_j(\xi, \zeta; Z)\}$ are assumed to be real smooth functions that vanish exponentially as $|\xi| \to \infty$. Counterpropagating solutions with a wavelength-scale $\zeta-$periodic grating characteristic are sought. Functions ψ_j are thus required to be $2\pi-$periodic in Z. Following general multiple-scales techniques, we assume that Z

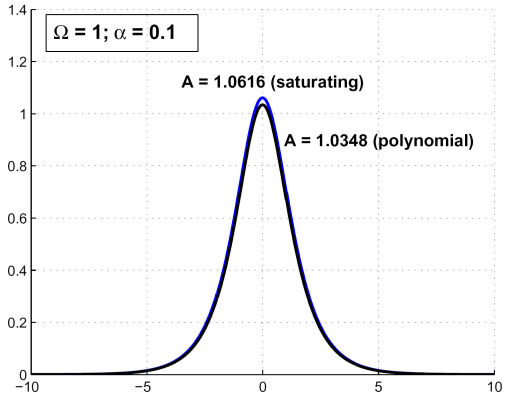

Figure 5: Transverse profiles $\psi_0(X)$ of localised counterpropagating solutions for two (related) nonlinearity functions. The value A refers to peak amplitude.

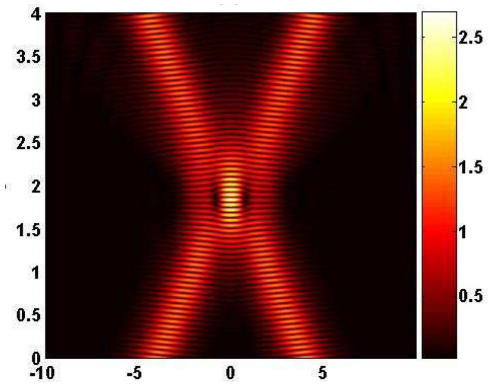

Figure 6: The interaction of counterpropagating Helmholtz solutions derived from full solution of Eq. (9), with $\kappa = 0.01, \Omega = 2, v = 2$ and a Kerr nonlinearity. The evolution of field amplitude $|\psi|$ is mapped out from $\zeta = 0$ to 4, within a transverse domain of $\xi = -10$ to 10.

is independent of ζ, and that $Z-$derivatives of the unknown functions are $\sim O(1)$ as $\kappa \to 0$.

By substituting Eq. (10) into Eq. (9) and equating terms at various powers of κ, it is straightfoward to see that the contribution at $O(\kappa^{-1})$ is identically zero due our choice of the cosine function in ansatz (10). At $O(\kappa^0)$, one finds

$$-\frac{1}{4}\left(\frac{\partial^2\psi_1}{\partial Z^2}+\psi_1\right) = A\cos\Theta + B\sin\Theta + \sum_{m=1}^{\infty} f_m(\psi_0^2)\psi_0\cos[(2m+1)\Theta], \qquad (11)$$

where the coefficients of the cos and sin terms are $A \equiv (\psi_0)_{XX} - (\phi_\zeta + \phi_\xi^2 + \phi_{\xi\xi})\psi_0 + f_0(\psi_0^2)\psi_0$ and $B \equiv (v - 2\phi_\xi)(\psi_0)_X - (\psi_0)_\zeta - \psi_0\phi_{\xi\xi}$, respectively,

$$f_m(s) = \sum_{n=m}^{\infty} \frac{F^{(n)}(0)}{n!}\begin{pmatrix} m+n+1 \\ 2n+1 \end{pmatrix}\left(\frac{s}{4}\right)^n, \qquad (12)$$

and $\begin{pmatrix} p \\ q \end{pmatrix}$ denotes a binomial coefficient. Periodic solutions to Eq. (11) exist only when $A = B = 0$.

It is consistent to seek particular solutions where $\phi(\xi,\zeta) = v\xi/2 + K\zeta$, and K is a constant. It then follows that ψ_0 must satisfy

$$\left(\frac{d\psi_0}{dX}\right)^2 = \Omega\psi_0^2 - \int_0^{\psi_0^2} ds f_0(s), \qquad (13)$$

where $\Omega = K + v^2/4$. The integral in Eq. (13) can be evaluated analytically for some specific nonlinearity functions, such as the dual power-law $f_0(\psi^2) = (p+1)\psi^{2p} - \alpha(2p+1)\psi^{4p}$. This includes Kerr nonlinearity when $p = 1$ and $\alpha = 0$, while for general p and α, one finds the solution

$$\psi_0(X) = \left[\frac{2\Omega}{1+\sqrt{1-4\alpha\Omega}\cosh(2p\sqrt{\Omega}X)}\right]^{1/2p}. \qquad (14)$$

Once $\psi_0(X)$ is known, it can be shown that

$$\psi_1(\xi,\zeta;Z) = C_1(\xi,\zeta)\cos\Theta + \sum_{m=1}^{\infty} f_m(\psi_0^2)\psi_0\frac{4\cos[(2m+1)\Theta]}{(2m+1)^2-1}, \qquad (15)$$

where the function $C_1(\xi,\zeta)$ is given by solvability conditions of the $O(\kappa^1)$ equations, and the $Z-$dependence on the right-hand-side of Eq. (15) is implicit within Θ.

It is also straightforward to employ numerical solution of Eq. (13) to determine the transverse profiles of counterpropagating solutions for a wider class of nonlinearities. Localised solutions for a saturating nonlinearity, $f_0(\psi^2) = 2\psi^2/(1+\alpha\psi^2)$, and its two-term polynomial approximation, $f_0(\psi^2) = 2\psi^2(1-\alpha\psi^2)$, are shown in Fig. 5.

Finally, we illustrate the solitonic character of the localised counterproagating solutions. Figure 6 shows a numerical solution of Eq. (9) involving two initially well-separated localised components. The form of each component is chosen to match ansatz (10) at $\zeta = 0$. Subsequent stable propagation and interaction, each exhibiting the wavelength-scale

oscillatory features in ζ, are mapped out vertically in this field-modulus plot.

Acknowledgements

This paper is dedicated to the late Dr. Valery E. Grikurov. His expertise and friendship will be dearly missed. Dr. Grikurov led our research on Helmholtz counterpropagation solitons during his visits to our laboratories in the University of Valladolid, Spain.

References

[1] Chamorro-Posada, P. & McDonald, G.S., 2006, Spatial Kerr soliton collisions at arbitrary angles, *Phys. Rev. E,* **Vol. 74**, art. no. 036609.

[2] Sánchez-Curto, J., Chamorro-Posada, P. & McDonald, G.S., 2007, Helmholtz solitons at nonlinear interfaces, *Opt. Lett.,* **Vol. 32**, pp. 1126–1128.

[3] Chamorro-Posada, P., McDonald, G.S. & New, G.H.C., 2002, Exact soliton solutions of the nonlinear Helmholtz equation: communication, *J. Opt. Soc. Am. B,* **Vol. 19**, pp. 1216–1217.

[4] Chamorro-Posada, P. & McDonald, G.S., 2002, Helmholtz dark solitons, *Opt. Lett.,* **Vol. 28**, pp. 825–827.

[5] Chi, S. & Guo, Q., 1996, Vector theory of self-focusing of an optical beam in Kerr media, 1995, *Opt. Lett.,* **Vol. 20**, pp. 1598–1600.

[6] Crosignani, B., Yariv, A. & Mookherjea, S., 2004, Nonparaxial spatial solitons and propagation-invariant pattern solutions in optical Kerr media, 2004, *Opt. Lett.,* **Vol. 29**, pp. 1254–1256.

[7] Joseph, R.M. & Taflove, A., 1994, Spatial soliton deflection mechanism indicated by FD-TD Maxwell's equations modelling, *IEEE Photon. Technol. Lett.,* **Vol. 6**, pp. 1251–1254.

[8] Newell, A.C. & Moloney, J.V., 1992, Nonlinear optics, Addison-Wesley.

[9] Chamorro-Posada, P, McDonald, G.S. & New, G.H.C., 2000, Propagation properties of nonparaxial spatial solitons, *J. Mod. Opt,* **Vol. 47**, pp. 1877–1886.

[10] Aceves, A.B., Moloney, J.V. & Newell, A.C., 1989, Theory of light-beam propagation at nonlinear interfaces. I. Equivalent-particle theory for a single interface, *Phys. Rev. A,* **Vol. 39**, pp. 1809–1827.

[11] Aceves, A.B., Moloney, J.V. & Newell, A.C., 1989, Theory of light-beam propagation at nonlinear interfaces. II. Multiple-particle and multiple-interface extensions, *Phys. Rev. A,* **Vol. 39**, pp. 1828–1840.

[12] Christian, J.M., McDonald, G.S. & Chamorro-Posada, P., 2007, Bistable Helmholtz solitons in cubic-quintic materials, *Phys. Rev. A,* **Vol. 76**, art. no. 033833.

[13] Hermann, J., 1992, Bistable bright solitons in dispersive media with a linear and quadratic intensity-depending refraction index change, *Opt. Commun.,* **Vol. 87**, pp. 161–165.

[14] Gatz, S. & Herrmann, J., 1992, Soliton collision and soliton fusion in dispersive materials with a linear and quadratic intensity-depending refraction index change, *IEEE J. Quantum Electron.,* **Vol. 28**, pp. 1732–1738.

[15] Haelterman, M., Sheppard, A.P. & Snyder, A.W., 1993, Bimodal counterpropagating spatial solitary-waves, *Opt. Commun.,* **Vol. 103**, pp. 145–152.

[16] Cohen, O., Uzdin, R., Carmon, T., Fleischer, J.W., Segev, M. & Odouov, S., 2002, Collisions between optical spatial solitons propagating in opposite directions, *Phys. Rev. Lett.,* **Vol. 89**, art. no. 133901.